Probing the Functional Role of Two Conserved Active Site Aspartates in Mouse Adenosine Deaminase†

Vera Sideraki,‡ Khalid A. Mohamedali,‡,§ David K. Wilson,|| Zengyi Chang,|| Rodney E. Kellems,⊥ Florante A. Quiocho,|| and Frederick B. Rudolph*,‡

Department of Biochemistry and Cell Biology and The Institute of Biosciences and Bioengineering, Rice University, Houston, Texas 77005, Howard Hughes Medical Institute and the Department of Biochemistry, Baylor College of Medicine, One Baylor Plaza, Houston, Texas 77030, and Verna and Mars McLean Department of Biochemistry, Department of Molecular and Human Genetics, Baylor College of Medicine, One Baylor Plaza, Houston, Texas 77030

Received December 11, 1995; Revised Manuscript Received March 27, 1996⊗

ABSTRACT: Two adjacent aspartates, Asp 295 and Asp 296, playing major roles in the reaction catalyzed by mouse adenosine deaminase (mADA) were altered using site-directed mutagenesis. These mutants were expressed and purified from an ADA-deficient bacterial strain and characterized. Circular dichroism spectroscopy shows the mutants to have unperturbed secondary structure. Their zinc content compares well to that of wild-type enzyme. Changing Asp 295 to a glutamate decreases the k_{cat} but does not alter the K_m for adenosine, confirming the importance of this residue in the catalytic process and its minimal role in substrate binding. The crystal structure of the D295E mutant reveals a displacement of the catalytic water from the active site due to the longer glutamate side chain, resulting in the mutant's inability to turn over the substrate. In contrast, Asp 296 mutants exhibit markedly increased K_m values, establishing this residue's critical role in substrate binding. The Asp 296 → Ala mutation causes a 70-fold increase in the K_m for adenosine and retains 0.001% of the wild-type k_{cat}/K_m value, whereas the Asp 296 → Asn mutant has a 10-fold higher K_m and retains 1% of the wild-type k_{cat}/K_m value. The structure of the D296A mutant shows that the impaired binding of substrate is caused by the loss of a single hydrogen bond between a carboxylate oxygen and N7 of the purine ring. These results and others discussed below are in agreement with the postulated role of the adjacent aspartates in the catalytic mechanism for mADA.

Adenosine deaminase (ADA,[1] EC 3.5.4.4) catalyzes the irreversible deamination of adenosine and 2′-deoxyadenosine to their respective inosine derivatives and ammonia. ADA is one of the enzymes involved in the purine metabolism pathway and is found in most mammalian tissues. It is indispensable to the upkeep of a competent immune system, since heritable deficiency of ADA is associated with severe combined immunodeficiency disease (SCID) (Hershfield & Mitchell, 1995). The change in enzyme levels is also observed in a number of other diseases such as anemia, various lymphomas and leukemias (Gan et al., 1987; Renouf et al., 1989; Kanno et al., 1988; Cowan et al., 1983), and acquired immunodeficiency syndrome. Recently, CD26, a molecule required for entry and infection of cells by the HIV virus, was shown to be identical to the ADA binding protein (Callebaut et al., 1993; Kameoka et al., 1993). A variety of 6-substituted purine derivatives and adenosine analogues will bind to the enzyme, but phosphorylated nucleosides are not substrates (Zielke & Suelter, 1971). Some of these compounds have seen clinical usage as antimetabolic and antineoplastic agents and as modulators of neurological function through their effects on adenosine levels (Glazer, 1980; Centelles et al., 1988).

ADA is a favorite candidate for mechanistic studies because it is a small, monomeric, easily purified enzyme that catalyzes a relatively simple chemical reaction with remarkable efficiency. The rate enhancement afforded to the reaction by the enzyme is on the order of 2×10^{12} (Frick et al., 1987). The reaction catalyzed by ADA appears to be encounter-limited (Kurz et al., 1992) with a k_{cat} of 375 s^{-1} and a k_{cat}/K_m of 1.4×10^7 M^{-1} s^{-1} (Frick et al., 1987). Several studies had previously suggested that the transition state of the reaction involves a tetrahedral intermediate at the C6 of the purine ring and identified sulfhydryl, histidyl, and carboxyl residues as the important groups in catalysis (Kati & Wolfenden, 1989; Kurz & Frieden, 1983; Weiss et al., 1987). More information on the mechanism for the reaction became available from the structure of murine ADA crystallized with purine riboside (Wilson et al., 1991). The inhibitor bound in the active site had undergone the first steps in the catalytic reaction to yield a hydrated adduct (HDPR, see Figure 2), presumably an analogue of the true tetrahedral intermediate. It also became apparent from the structure that there was a catalytically active zinc bound in the enzyme's

† This work was supported by Grants GM 42436 (F.B.R. and R.E.K.) and DK 46207 (R.E.K.) from the National Institutes of Health and Grant C-1041 (F.B.R.) from the Robert A. Welch Foundation and in part by the Howard Hughes Medical Institute (F.A.Q.).

* Corresponding author: Dr. Frederick B. Rudolph, Department of Biochemistry and Cell Biology, P.O. Box 1892, Houston, TX 77521-1892. Telephone: 713-527-4017. Fax: 713-285-5154.

‡ Rice University.

§ Present address: Department of Pathology, Baylor College of Medicine, One Baylor Plaza, Houston, TX 77030.

|| Howard Hughes Medical Institute and the Department of Biochemistry, Baylor College of Medicine.

⊥ Verna and Mars McLean Department of Biochemistry, Department of Molecular and Human Genetics, Baylor College of Medicine.

⊗ Abstract published in *Advance ACS Abstracts,* June 1, 1996.

[1] Abbreviations: ADA, adenosine deaminase; SCID, severe combined immunodeficiency disease; ss DNA, single-stranded DNA; IPTG, isopropyl β-D-thiogalactopyranoside; CD, circular dichroism; FAAS, flame atomic absorption spectroscopy; N6MA, N_6-methyladenosine; PR, purine riboside; HDPR, 6(*R*)-hydroxy-1,6-dihydropurine ribonucleoside.

S0006-2960(95)02920-5 CCC: $12.00

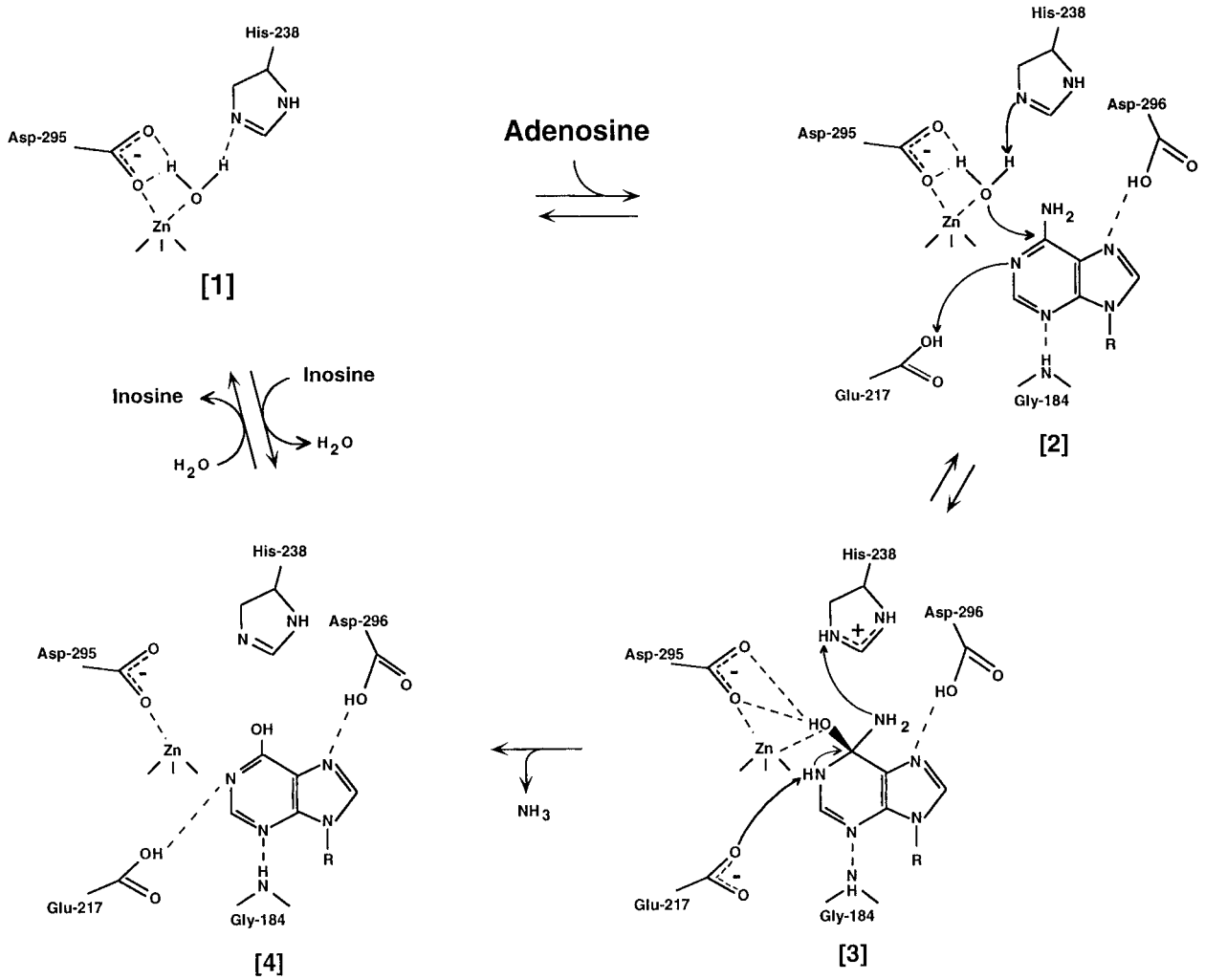

FIGURE 1: Schematic diagram of the mechanism for the reaction catalyzed by adenosine deaminase. Dashed lines indicate noncovalent interactions between neighboring atoms. (Step 1) The zinc cofactor is coordinated to three His residues (not shown), Asp 295, and the catalytic water. The water is oriented for attack by hydrogen bonds to His 238 and Asp 295. (Step 2) His 238 abstracts the proton from the catalytic water, and the hydroxylate attacks the substrate's C6; the N1=C6 double bond is lost, and N1 becomes protonated by Glu 217. Also shown are Asp 296 and Gly 184, donating hydrogen bonds to N7 and N3, respectively. (Step 3) The tetrahedral intermediate collapses with the amino group becoming protonated, possibly by His 238, and leaving in the form of ammonia. (Step 4) The enol form of the product inosine is shown bound to the active site.

active site. From this and a second crystal structure (Wilson & Quiocho, 1993) of murine ADA bound to the ground-state analogue 1-deazaadenosine, the following S_N2 mechanism was proposed (Figure 1). The zinc cofactor activates a liganded water molecule from which the nearby His 238 abstracts a proton, thus creating the attacking hydroxyl group. The incipient hydroxyl is oriented for attack on the C6 of the substrate through its interaction with Asp 295, His 238, and the zinc. Asp 295 is thought to hydrogen bond to the catalytic water and share a zinc ligand site with it. The protonated Glu 217 facilitates the reaction by donating a hydrogen bond to N1 of the purine, thus enabling the formation of a tetrahedral C6 (Mohamedali et al., 1996). The source of the proton added to the amino leaving group is still in question, with His 238 being a possible candidate. Residues Asp 296 and Gly 184 participate in hydrogen bonds with N7 and N9 of adenosine, respectively, thus reducing the aromaticity of the purine ring and facilitating nucleophilic attack at C6 (Figure 1).

The two neighboring aspartates, Asp 295 and Asp 296, are conserved in *Escherichia coli*, and mouse ADA (Chang et al., 1991). The crystallographic data clearly implicate Asp 295 as being important in catalysis since it occupies a zinc ligand site together with the catalytic water and three histidines and helps to correctly orient this water for deprotonation by His 238 and attack on C6 of the substrate. Asp 296 on the other hand is important in substrate binding because it is coplanar with the purine ring and it donates a hydrogen bond to N7 of the substrate (Figure 1). We initiated site-directed mutagenesis studies in order to examine the proposed roles of these two residues. The anchoring of the catalytic water by Asp 295 was probed by changing the residue into a Glu (D295E), whereas the hydrogen-bonding ability of Asp 296 with N7 was examined in Ala (D296A) and Asn (D296N) mutants. The mutants were purified and characterized by enzyme kinetic and structural studies. The D295E and D296A mutants were crystallized, and our kinetic data correlated with information from these structures. These combined results indicate that Asp 295 plays a critical role in catalysis through its interaction with the catalytic water, whereas Asp 296 is required for proper binding of the substrate in the active site.

MATERIALS AND METHODS

Bacterial Strains and Vectors. The mouse adenosine deaminase cDNA was inserted in the pRC4 phagemid expression vector under control of an IPTG-inducible tac promoter (Chang et al., 1992). The F1 locus on this vector allows for superinfection with IR1/M13 helper phages and isolation of single-stranded (ss) DNA. Bacterial strains CJ236 and BW313 were used for the production of uridine-rich ss DNA. A third *E. coli* strain, 71-18, was used for mutant selection and plasmid propagation. Mutant plasmids were expressed in the ADA$^-$ strain SΦ3834 (Chang et al., 1991). Both the pRC4 vector and the SΦ3834 strain were developed in Dr. Rodney Kellems' laboratory at Baylor College of Medicine, Houston.

Site-Directed Mutagenesis. The Kunkel method for producing site-specific mutants was followed (Kunkel et al., 1987). Uridine-rich ss DNA was isolated from pRC4-transformed CJ236/BW313 cells (*dut*$^-$ *ung*$^-$ genotype). The appropriate mutagenic primers were annealed onto the template ss DNA, and the second strand was synthesized using the Muta-Gene M13 *in vitro* Mutagenesis Kit (Bio-Rad). The synthesized double-stranded DNA products were transformed into a wild-type strain (71-18) and selected on LB-ampicillin plates. ss DNA from individual colonies was isolated and sequenced in the area of the mutation (Sequenase kit, United States Biochemicals). Once mutant colonies were identified (only 15−25% of all colonies), the entire cDNA was sequenced to ensure that no other alterations were present.

Protein Expression and Purification. Wild-type and mutant plasmids were expressed in the ADA$^-$ strain SΦ3834. Overnight cultures were inoculated into 6 L of superbroth medium (32 g/L bactotryptone, 20 g/L yeast extract, and 5 g/L sodium chloride) containing 1 mM zinc sulfate and 60 mg/mL ampicillin. Ten hours into the growth, 4 mg/L IPTG (Sigma) was added, and growth was continued for 20 h. The cells were harvested and frozen at −20 °C. Cell pellets from the entire 6 L culture were resuspended in 80 mL of DEAE buffer [50 mM imidazole (pH 6.8), 10 μM zinc sulfate, 5% glycerol, and 1 mM dithiothreitol] containing 1 mM AEBSF protease inhibitor (Sigma). A French Pressure Cell (SLM Instruments) was used for cell lysis, and the resulting homogenate was centrifuged at 100000*g* for 1 h in a Beckman L5-50 ultracentrifuge using a 55.2 rotor. The supernatant was loaded onto a DEAE-cellulose column (5 × 10 cm, Whatman) and eluted using a 0 to 0.5 M NaCl salt gradient in DEAE buffer. Fractions were collected at a flow rate of 1 mL/min. The ADA proteins eluted between 12 and 17 h into the gradient. ADA-containing fractions were determined by spectrophotometric assays (as described below), pooled, and brought to 60% saturation with ammonium sulfate. After centrifugation, the supernatant was saturated to 80% with ammonium sulfate and centrifuged. The pellet was dissolved in 70% HIC buffer [20 mM potassium sulfate (pH 7.0), 10 μM zinc sulfate, 5% glycerol, and 1 mM dithiothreitol] containing 2 M ammonium sulfate and loaded onto a hydrophobic interaction HPLC column (Polypropyl A, 5 μM, Custom LC, Inc.). Proteins were eluted with HIC buffer at a flow rate of 1 mL/min. The eluate was monitored at 280 nm, and the ADA peak typically eluted at 30 min. The ADA-containing fractions were concentrated by dialysis overnight against 20% PEG (molecular weight of 15000−20000) (Sigma) in AX300 buffer [20 mM imidazole (pH 6.8), 10 μM zinc sulfate, 5% glycerol, and 1 mM dithiothreitol]. The dialysate was washed with 75% AX300 buffer, loaded onto a silica-based polyethyleneimine HPLC column (SynChropak AX300, 10 × 250 mm, Synchrom, Inc., and eluted with AX300 buffer containing 500 mM sodium chloride. The ADA peak eluted at 25−30 min at a flow rate of 1 mL/min. The purified protein was concentrated in Tris-Zn buffer [10 mM Tris-HCl (pH 7.0), 10 μM zinc sulfate, 50% glycerol, and 1 mM dithiothreitol] and stored in air-tight vials under argon at −20 °C. All purification steps except HPLC were performed at 4 °C.

SDS−Polyacrylamide Gel Electrophoresis and Western Blots. SDS−polyacrylamide gel electrophoresis was performed according to the method of Laemmli (1970) on a minigel apparatus (Bio-Rad). Proteins were stained with Coomassie Brilliant Blue. The Rainbow molecular weight markers (Amersham Corp.) were used as standards. For Western blots, proteins separated by SDS−PAGE were blotted onto Immobilon-P transfer membranes (Millipore). The primary antibody was goat anti-mADA polyclonal antibody, and the secondary was alkaline phosphatase-conjugated rabbit anti-goat IgG (Sigma Immunochemicals). Protein concentrations were determined by the method of Bradford (1976) using bovine serum albumin as standard and the Bio-Rad Protein Assay Reagent.

Enzyme Assays and Kinetic Analyses. Enzymatic activities were assayed on a Cary 118 spectrophotometer by measuring the rate of ADA-dependent increase of inosine absorption at 235 nm at 30 °C, using an extinction coefficient of 3.5 mM^{-1} cm^{-1}. One unit of ADA activity is defined as the amount of enzyme that produces 1 μmol of inosine per minute. Cuvettes with a 1 cm (for the wild-type and D295E enzymes) or 0.2 cm path length (for the Asp 296 mutants) were used. Assays were carried out in 50 mM potassium phosphate buffer (pH 7.2). Activities were measured over at least six different concentrations of adenosine, and the assays were repeated at least three times. For D295E, D296N, and wild-type ADA, adenosine concentrations ranged from 0.5 to 5 × K_m. For D296A, an alternative assay was used (see below). The concentration of enzyme in the assay mixture ranged from 0.1 nM for the wild-type to 0.3 μM for the least active mutant. Kinetic parameters were determined by Lineweaver−Burke plots with a fourth power weighting function using the Enzyme Kinetics (Trinity Software) program. K_i values for two ADA inhibitors, N_6-methyladenosine (N6MA) and purine riboside (PR), were determined for the enzymes. Assays were performed as above, with thorough mixing of the substrate and inhibitor in the reaction mixture prior to addition of the enzyme. Two to four different inhibitor concentrations bracketing the K_i value were used in the assays, and each velocity vs substrate curve was determined at least three times. Inhibition plots and K_i values were obtained as described above. The kinetic parameters K_m and k_{cat} refer to the following mechanism for a one-substrate reaction:

$$E + A \underset{k_{-1}}{\overset{k_1}{\rightleftharpoons}} EA \xrightarrow{k_2} E + P$$

where A is adenosine and E is ADA, and $K_m = (k_{-1} + k_2)/k_1$. Kurz et al. (1992) calculated the individual rate constants for the hydrolysis of adenosine by calf intestine ADA. From

their data, K_m was not equal to the dissociation constant (k_{-1} was predicted from their data to be close to zero, k_1 was 11 μM^{-1} s^{-1}, and k_2 was 246 s^{-1}). By contrast, Porter and Spector (1993) calculated K_m (24 μM) to be close to the dissociation constant (16 μM) with a k_{-1} value close to 500 s^{-1}, k_1 equal to 31 μM^{-1} s^{-1}, and k_2 equal to 244 s^{-1}. In the present study, we assume that the value for K_m is not equal to K_d for the wild-type; with our less active mutants, k_2 is extremely low, and K_m approaches K_d. For the determination of the K_m, k_{cat}, and K_i values of D296A, an ammonia detection assay was used. The amount of ammonia produced from the ADA-dependent adenosine deamination was measured on a Cary 118 spectrophotometer at 400 nm at 30 °C. Reaction mixtures contained 0.625−5 mM adenosine, 0.8 μM D296A, and either 1.5 and 2.5 mM N6MA or 5 and 7.5 mM PR in 50 mM potassium phosphate buffer (pH 7.4). Reaction mixtures were incubated at 30 °C for 8 min (control experiments determined linearity of the reaction between 2 and 12 min), and then the reactions were stopped by the addition of 30 μL of Ammonia Color Reagent (Sigma). Their absorbance at 400 nm was recorded and converted to the amount of ammonia produced using a standard curve for absorbance at 400 nm by a range of ammonium sulfate concentrations from 12.5 to 200 μM. Kinetic parameters were calculated from rates plotted against substrate levels using the Enzyme Kinetics program as described above.

pH Dependence Studies. pH profiles for the four enzymes were determined over the range of pH 4−10 using the following buffers: 50 mM sodium acetate (pH 4 and 5.5), 50 mM potassium phosphate (pH 7.0), and 50 mM glycine (pH 8.5 and 10). The ionic strength of each buffer was adjusted to 0.1 with potassium sulfate. Reaction rates were measured by performing the enzyme assays in triplicate in each buffer at five different substrate concentrations.

Circular Dichroism Spectroscopy. CD spectra were measured in the far-UV (200−260 nm) and the near-UV (260−340 nm) region on an Aviv 6100 Spectrometer at Dr. John S. Olson's laboratory, Rice University. Measurements were made using a 0.02 cm path length cuvette (Starna Cells, Inc.). Each scan was recorded in 1 nm increments at 25 °C, repeated three times, and averaged. The proteins were in 20 mM Hepes buffer (pH 7.0), and their concentration was adjusted to 1 mg/mL prior to spectral acquisition. Protein concentration assays were done to determine the exact amount of enzyme in each sample. The spectrum of the buffer was subtracted from all protein spectra, and the observed ellipticities, θ, were normalized for protein concentration.

Flame Atomic Absorption Spectroscopy. Flame atomic absorption spectroscopy (FAAS) was performed on a Perkin-Elmer 2380 Atomic Absorption Spectrophotometer at the laboratory of Dr. David Giedroc, Texas A&M University, College Station, TX. The absorption of protein samples at 213.9 nm (λ characteristic for zinc) was measured using seven zinc nitrate solutions (from 0.5 to 8 μM concentration) as standards. All protein samples were extensively dialyzed in metal-free dialysis tubing (Auld, 1988) against metal-free 20 mM Hepes buffer (pH 7.0) prepared by passage through a Chelex-100 (Sigma) column. The dialysis buffer was changed three times during the experiment. Protein concentrations were between 2 and 6 μM. Measurements for each sample were taken twice, background-subtracted, and averaged.

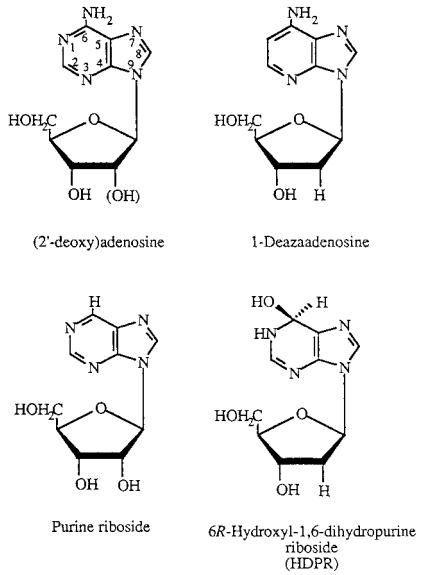

FIGURE 2: Chemical structures of substrates and inhibitors of adenosine deaminase. Crystal structures of mouse adenosine deaminase were grown in the presence of the inhibitor purine riboside, which can be bound as its hydrated adduct, HDPR. 2′-Deoxyadenosine is the natural substrate; 1-deazaadenosine is a weak substrate.

Fluorescence Spectroscopy. Fluorescence spectroscopy was performed on a SLM 8100 spectrofluorimeter at the laboratory of Dr. John S. Olson, Rice University. The excitation wavelength used was 290 nm, and the emission was scanned from 300 to 400 nm. Measurements were made using a 1 cm path length fluorescence cuvette (Starna Cells, Inc.). Samples of 1 μM ADA were in 100 mM potassium phosphate buffer (pH 7.5).

Crystallography. Crystals of the mutant ADAs were grown in the presence of purine ribonucleoside (Figure 2) as described before (Wilson et al., 1991). These were then harvested into a solution containing 10.5% polyethylene glycol 6000 and 50 mM sodium citrate (pH 4.2) and mounted in thin-walled capillaries for data collection. Intensities were collected on an ADSC multiwire area detector mounted on a Rigaku RU-200 generator operated at 40 kV and 110 mA. To minimize radiation damage during data collection, crystals were cooled to 4 °C. Crystal parameters and statistics for each data set are summarized in Table 3.

Crystals belonged to space group *C*2, and since they were isomorphous with those of the wild-type enzyme complexed with HDPR, refinement commenced using this structure as a starting point. In order to determine the nature of the bound inhibitor and the position of the glutamate side chain in the D295E mutant, the inhibitor was removed from each model and each mutated position was changed to an alanine. Water molecules from the wild-type structure were included and later removed if the associated ($2|F_o| - |F_c|$, α_c) density did not appear after refinement when contoured at 1σ. The structures were then subjected to positional and temperature factor refinement using XPLOR (Brünger, 1992) before ($|F_o| - |F_c|$, α_c) maps were calculated. These maps showed density corresponding to purine riboside in the active site of the D295E mutant and HDPR in the D296A mutant. Each structure was fit with its respective inhibitor. The conformation of the Glu 295 side chain was also determined using this unbiased density and fit accordingly. At this point, each structure and corresponding ($2|F_o| - |F_c|$, α_c) and ($|F_o| -$

Table 1: Purification Scheme of D295E

step	volume (mL)	total activity (units[a])	total protein (mg/mL)	specific activity (unit/mg)	purification factor	yield (%)
crude extract	100	27	135	0.002	1	100
DEAE-cellulose	181	4	4	0.006	3	15
ammonium sulfate (60−80%)	8	3.6	28	0.016	8	13
HIC HPLC	16	2.4	3	0.050	25	9
PEG dialysate	8	3	5	0.080	40	11
AX300 HPLC	10	3	2.3	0.130	65	11

[a] One unit of activity is defined as the amount of enzyme that produces 1 μmol of inosine per minute.

$|F_c|$, α_c) density were examined in their entirety and minor adjustments were made. A final cycle of positional and temperature factor refinement yielded the final structures. Refinement results are shown in Table 3. The Protein Data Bank entry numbers are as follows: D295E, 1FKW; D296A, 1FKX.

RESULTS

Protein Expression and Purification. The three mutant mADA plasmids were constructed and identified by sequencing. They were sequenced in their entirety to confirm integrity of the mADA cDNA outside the area of the mutation. Expression of tne mutants in the ADA$^-$ strain SΦ3834 after induction with IPTG yielded from 20 mg of pure protein for the D295E mutant to 160−200 mg for the Asp 296 mutants from the 6 L cultures. The wild-type ADA yield from the same culture volume was 100 mg on average. The growth medium was supplemented with extra zinc to avoid low protein production from the bacteria due to limiting amounts of the cofactor. The D295E, D296N, and D296A mutants eluted from the DEAE column step at times similar to those for the wild-type. With the D295E mutant, about 80% of the enzymatic activity was lost during the DEAE column step (Table 1). Efforts to retrieve the mutant from different fractions of the column were fruitless and gave evidence that this sample was unstable, breaking down during this step. The remaining D295E, the Asp 296 mutants, and the wild-type eluted at similar times during hydrophobic and AX300 ion-exchange column chromatography. The general uniformity of elution characteristics among wild-type and mutant ADAs was taken as preliminary evidence that the expressed proteins were correctly folded. All ADA proteins were clearly detected by activity assays as early as the DEAE column step.

We observed two peaks with differing stabilities and activities at the HIC and AX300 column steps if reducing agents were omitted from the purification, presumably reflecting reduced and oxidized forms of the enzymes. Therefore, reducing agents, additional zinc, and glycerol were faithfully included in each purification step to minimize oxidation, zinc loss, and overall misfolding of the proteins. The purified proteins appear as single bands on SDS−PAGE gels with a molecular weight of about 40 000; a few faint bands of lower molecular weight were also observed on the gels in some cases. Western blots showed that these bands correspond to degradation products of ADA, which may be arising during purification and subsequent electrophoresis (data not shown). SDS−PAGE gels of mutant proteins at later time points following purification and storage did not exhibit an increase in the amount of the degradation product, underlining the stability of the pure samples under our storage conditions. Purified samples were kept in a Tris-zinc−50% glycerol−DTT buffer at −20 °C under an argon atmosphere and remained stable for more than 6 months. The overall yields and high degree of purity of the mutants are an indication of the success of our purification protocol, which sidesteps the use of affinity chromatography when purifying mutants with altered substrate binding characteristics or small differences in tertiary folding.

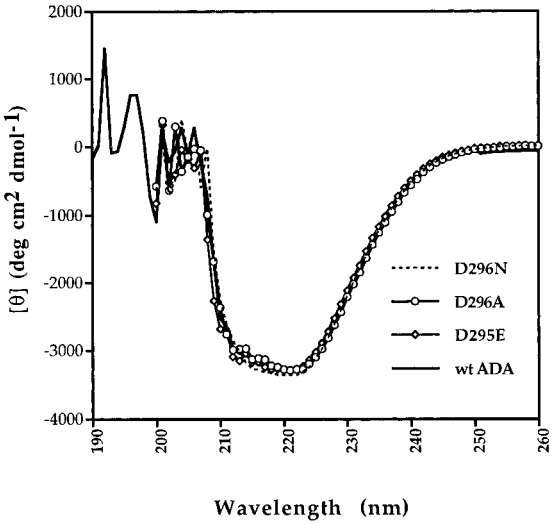

FIGURE 3: Far-UV CD spectra of wild-type and mutant ADA (25 μM protein in 20 mM HEPES buffer at pH 7.0). Each spectrum is the average of three scans. No attempt was made to fit the data. All spectra were normalized for protein concentration (see Materials and Methods).

Evaluation of Secondary Structure of ADA by Circular Dichroism. To examine whether the presence of each mutation had disrupted the overall enzyme structure, circular dichroism spectroscopy was performed. The spectrum of wild-type mADA exhibits the double minima at 208 and 222 nm characteristic of α-helical content and a minimum at 218 nm reflecting β-sheet structure (Adler et al., 1973). The CD spectra of all three ADA mutants are virtually indistinguishable from that of the wild-type protein (Figure 3). This confirms that the mutated sites did not result in alterations of ADA's overall secondary structure.

Evaluation of Tertiary Structure of ADA by Fluorescence and Near-UV Circular Dichroism. To examine the possibility that our mutations had resulted in disruption of the local environment around the enzyme's four tryptophans, the intrinsic fluorescence spectra of wild-type and mutant ADAs were obtained (Figure 4). In good agreement with that of calf intestine (Kurz et al., 1985) and human thymus adenosine deaminase (Philips et al., 1987), tryptophan emission in murine ADA exhibits a maximum at 330 nm in spectra of the wild-type and mutant enzymes. The maximal intensities differ by less than 10%. All four spectra are similar, indicating that the protein regions surrounding the tryptophan

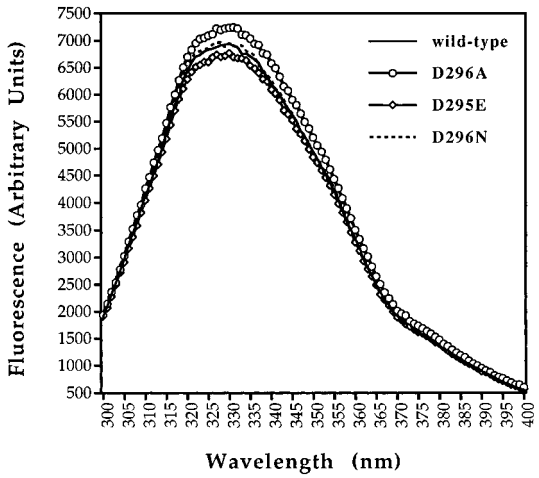

FIGURE 4: Fluorescence emission spectra of wild-type and mutant ADA (1 μM protein in 100 mM potassium phosphate buffer at pH 7.5). An excitation wavelength of 290 nm was used (see Materials and Methods).

residues have not sustained major changes as a result of the mutated sites. Similarly, the 260−340 nm CD spectra of the mutants could be superimposed on the spectrum of the wild-type enzyme and show an overall conservation of the tertiary fold (data not shown).

Zinc Content of ADA. In order to ascertain that the ability of our mutants to bind zinc was not affected, the zinc content of mutant and wild-type ADA was measured by FAAS after extensive dialysis (18 h) of the proteins in zinc-free buffer. The amount of zinc in the final buffer was measured and subtracted from that of the samples. The ratios of zinc to enzyme for the mutants are comparable to those for the wild-type mADA. All ratios, including that of the wild-type, were 30−40% lower than the expected 1:1 ratio (data not shown). To test for possible denaturation of the proteins and concomitant loss of zinc during the long dialysis step, the enzyme activities of the wild-type and the mutants were tested before and after dialysis. We saw a 30% drop in activity as a result of the dialysis step, which correlates to the 30% drop in the metal:protein ratios, suggesting that denaturation was the cause for the observed zinc loss. These results confirm that our mutations do not impair ADA's ability to bind zinc.

Kinetic Properties of Mutants. To examine the effect of our mutations on the kinetic parameters of the enzyme, k_{cat}, k_{cat}/K_m, and K_m values for adenosine for mutant and wild-type ADAs were obtained (Table 2). All mutants have greatly impaired catalytic efficiencies (k_{cat}/K_m) compared to the wild-type enzyme. The most active of the mutants, D296N, has a k_{cat}/K_m of 1%, while D295E and D296A retain 0.04 and 0.001% of the wild-type catalytic efficiency, respectively. Differences among the three mutants in their ability to bind the substrate are seen. While the D295E mutant has a K_m for adenosine comparable to the wild-type value, mutations at residue 296 cause dramatic decreases in substrate affinity. Thus, the *K3m* value for adenosine for D296N is 10-fold higher than that for wild-type, and for the D296A mutant 70-fold higher. These findings support the minimal role of Asp 295 in substrate binding and stabilization and corroborate the theory that Asp 296 is essential in anchoring the substrate to the active site.

Inhibition of Mutant Enzymes. Inhibition constants for two of the mutants (D295E and D296N) and wild-type mADA were measured by inhibition assays at 235 nm using two substrate analogues, purine ribonucleoside and N_6-methyladenosine. Both compounds are competitive inhibitors with respect to adenosine for all three ADAs. As expected from the results of the substrate binding assays, the K_i values for both inhibitors with the D295E mutant were similar to those for the wild-type enzyme, reinforcing the finding that Asp 295 does not participate in substrate or inhibitor binding. The K_i values for D296N were sharply increased, with the K_i for N_6-methyladenosine being 14-fold higher and the K_i for purine ribonucleoside 160-fold higher than that for wild-type. Inhibition values for D296A were measured using the ammonia detection assay. The K_i value for N6MA with D296A was, as expected from the mutant's high K_m value, 175 times higher than the wild-type inhibition constant; its K_i value for PR was even greater, approximately 700 times higher than the wild-type K_i (Table 2). Both substrate analogues were competitive inhibitors of the enzyme with respect to adenosine.

pH Profiles of Wild-Type and Mutant Enzymes. The pH dependence for the reaction catalyzed by ADA is a bell-shaped curve, with an acidic pK_a of about 5 and a basic pK_a of 9. If either of the two aspartates were responsible for one of the pK_a values, our mutants might be expected to have different pH profiles compared to the wild-type enzyme. To examine this possibility, we measured the mutants' steady-state kinetic parameters at different pH values. The pH profiles for the k_{cat} and k_{cat}/K_m values of wild-type and mutant ADAs are shown in Figure 5. The same pH dependence is seen with both profiles of D295E and D296A. Both the k_{cat} and k_{cat}/K_m of D296N have somewhat higher values at pH 5.5, and the free enzyme D296N pH profile has a slightly lower basic pK_a of about 8 (Figure 5B). Control experiments where all four enzymes were incubated in buffers of pH 4.0−10.0 for the duration of a typical assay (4−5 min) and then assayed at pH 7.2 showed that the activity drop at the extremes of the pH range is not caused by denaturation of the enzymes (data not shown). All three mutants and the wild-type enzyme retained 80−100% of their activity after incubation at pH 4.0−10.0. Overall, these data suggest that our mutations at residues 295 and 296 do not significantly alter the pH dependence of the ADA reaction under steady-state conditions.

Crystallography. The crystal structures of D295E and D296A were solved using purine riboside as the inhibitor. When this substrate analogue is used to grow ADA crystals, the catalytic water attacks C6 to form 6(*R*)-hydroxy-1,6-dihydropurine ribonucleoside (HDPR, see Figure 2). The reaction then stalls at this point due to the lack of a leaving group. The resulting complex, which would dehydrate very quickly in solution (Jones et al., 1989), is stable within the confines of the active site for the weeks in which it takes to grow the crystals and collect the data.

The crystals of D295E showed that, while the overall structure was not perturbed, the inhibitor that was bound to the protein was PR and not HDPR (Figure 7). An activated water molecule, poised to attack as in the case of the wild-type structure complexed with 1-deazaadenosine (Wilson et al., 1993), was not observed. Instead, the extra methylene in the glutamate side chain has caused its carboxylate group to displace the catalytic water which is liganded to the zinc in wild-type ADA. The glutamate still chelates the zinc but makes contacts with the purine ring which is displaced by

Table 2: Kinetic Parameters of Wild-Type and Mutant ADA

sample	K_m[b] (μM)	k_{cat}[b] (s^{-1})	k_{cat}/K_m (μM^{-1} s^{01}(	K_i[b] (μM) PR	K_i[b] (μM) N6MA
wild-type	21 ± 2	240 ± 20	11	9 ± 2	12 ± 1
D295E	26 ± 2	0.11 ± 0.01	0.004	9 ± 2	15 ± 4
D296A	1400 ± 400[c]	0.17 ± 0.02[c]	0.0001	6000 ± 2000[c]	2100 ± 600[c]
D296N	200 ± 10	17 ± 1	0.11	1440 ± 40	170 ± 20

[a] Assays were performed at 30 °C in 50 mM phosphate buffer (pH 7.2) with adenosine as the substrate (see Materials and Methods). [b] Averages of at least three separate determinations. [c] Measured using an ammonia detection assay (see Materials and Methods).

Table 3: Crystallographic Data and Refinement Statistics

parameter	D295E	D296A
resolution (Å)	2.4	2.4
reflections (measured/unique)	40777/24014	25228/15662
used in refinement ($I \geq \sigma I$)	18 210	13 684
R_{merge}	0.051	0.042
unit cell	$a = 102$ Å $b = 94$ Å $\beta = 127°$ $c = 73$ Å	$a = 102$ Å $b = 94$ Å $\beta = 127°$ $c = 73$ Å
R factor	0.176	0.170
rms deviation from ideal bond distance (Å)	0.013	0.012
rms deviation from ideal angle (deg)	1.71	1.68
B factor (main chain)	20.94	20.00
B factor (side chain)	24.11	22.88
number of water molecules	69	60

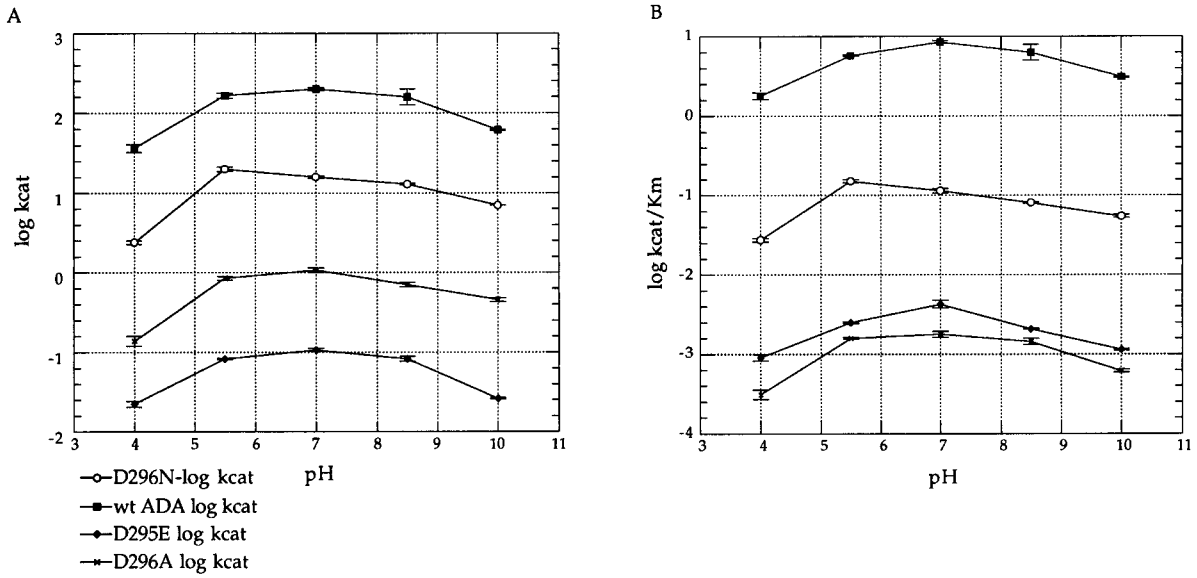

FIGURE 5: pH dependence of the k_{cat} (A) and k_{cat}/K_m (B) of mutant and wild-type ADA with adenosine as the substrate. Points represent averages of three separate kinetic value determinations. No attempt has been made to fit the data.

approximately 0.50 Å relative to the wild-type structure. The displaced purine ring no longer engages in hydrogen bonding to Oϵ1 of Glu 217 via N1. Without this interaction, the side chain of Glu 217 adopts a different conformation.

The crystal structure of D296A (Figure 8) is generally similar to that of the wild-type enzyme (Figure 6). When superimposed on each other, the two active sites show no substantial differences in the positions of their amino acids or the zinc cofactor. The plane of the purine ring in D296A is, however, shifted slightly by approximately 0.40 Å, which may be a direct consequence of the lack of the hydrogen bond to N^- due to the mutation. Examination of the electron density in the active site shows that the purine riboside, which was included in the crystallization, is bound as an adduct at the 6 position. These results agree with the increased K_m and K_i values observed with D296A in our kinetic studies and confirm the proposed role of this residue in substrate binding.

DISCUSSION

The two adjacent aspartates in adenosine deaminase have been conserved in bacterial as well as mammalian ADA sequences (Chang et al., 1991). This immediately suggested that they may play important roles in the function of the enzyme. The discovery that both aspartates lie in the active site and interact with the substrate, the zinc cofactor, and the catalytic water strengthened this theory (Wilson et al., 1991). Our results with mutants of Asp 295 and 296 clearly demonstrate that both residues are essential for proper catalytic function.

Changing Asp 295 to Glu has no effect on either the enzyme's K_m value for adenosine or the inhibition constants

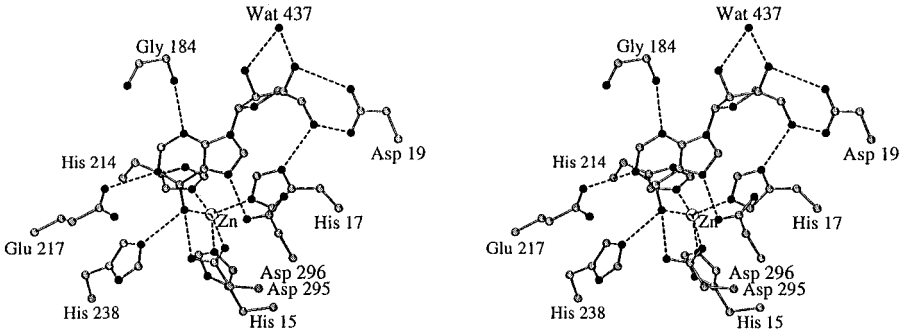

FIGURE 6: Stereoscopic view of the wild-type active site complexed to HDPR. Dashed lines indicate noncovalent interactions between neighboring atoms. One of the Asp 295 carboxylate oxygens is coordinated to the zinc, and the other interacts with the C6 hydroxyl. Asp 296 is coplanar with the purine ring and makes a hydrogen bond contact with N7.

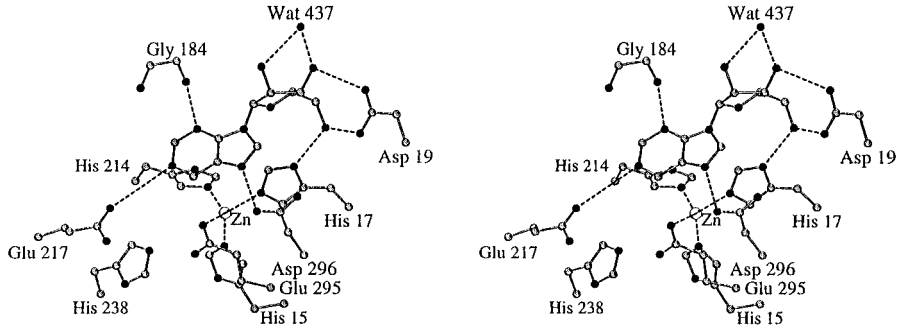

FIGURE 7: Stereoscopic view of the D295E mutant complexed to purine riboside. The Glu 295 has displaced the catalytic water from the vicinity of the zinc. One of the Glu 295 carboxyl oxygens provides the fourth zinc ligand. The purine ring is displaced by 0.5 Å relative to its position in the wild-type active site. The Glu 217 is also displaced and is now too far from the optimal hydrogen-bonding distance with N1 of the inhibitor.

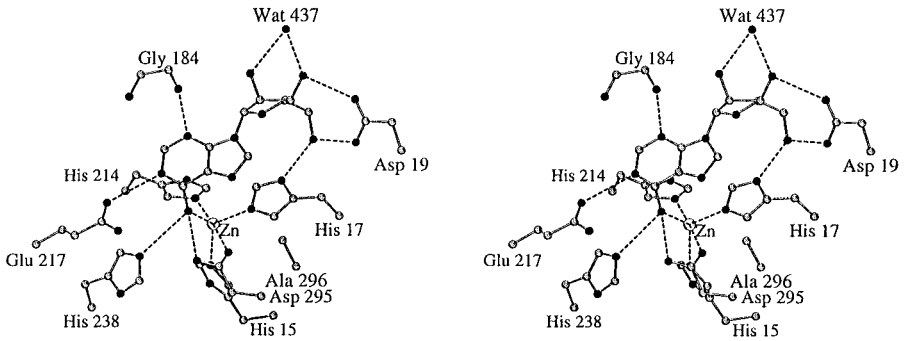

FIGURE 8: Stereoscopic view of the D296A mutant complexed to HDPR. The new Ala 296 results in the loss of the hydrogen bond with N7 of the purine. The purine ring is displaced by 0.4 Å relative to its position in the wild-type active site.

for the two substrate analogues, N_6-methyladenosine and purine riboside (Table 2). This agrees with the hypothesis that Asp 295 is not involved directly in binding the substrate or inhibitor in the active site (Wilson et al., 1991; Wilson & Quiocho, 1993). The mutation, however severely compromises the enzyme's catalytic effeiciency, since the k_{cat}/K_m value is only 0.04% of the wild-type value. The D295E crystal structure supports and explains these kinetic results, showing the enzyme to be bound to the inhibitor purine riboside instead of the hydrated adduct HDPR (Figure 7). this mutant is largely inactive because the catalytic water (source of the attacking hydroxyl group) is displaced from the active site by the longer side chain of Glu 295. No other changes have occurred in the mutant active site, barring a slight shifting in the position of the purine ring and Glu 217; thus, substrate or inhibitor binding is not affected. In solution, it must still be possible, albeit rare, for a water molecule to bind the active site and fit as a ligand to the zinc, perhaps displacing the glutamate at position 295 or minimizing this ligand's interaction with the metal cofactor. Since the essential catalytic residues such as His 238 and Glu 217 are still in place, this water molecule can be activated and reaction can occur. The rare binding of a water in solution and subsequent catalysis are the origin of the D295E mutant's small, non-zero k_{cat}/K_m value.

In contrast to those for D295E, substrate and inhibitor affinities for the Asp 296 mutants are dramatically decreased as compared to those for the wild-type enzyme. The change from an aspartate to an asparagine at position 296 results in a 10-fold increase in the K_m value for adenosine, a 14-fold increase in the K_i value for N_6-methyladenosine, and a 160-fold increase in the K_i for purine riboside. Changing Asp 296 to an alanine results in extremely low affinities for adenosine, with a K_m at least 70-fold higher than that of the wild-type enzyme. Inhibition studies with this mutant show increases in the K_i values for both inhibitors, with the value for N6MA being approximately 2 mM, 175 times higher than the wild-type inhibition constant. The K_i value for purine riboside is, as we also observe with the D296N mutant, even more dramatically increase (6 mM) and is now 700 times

higher than the wild-type ADA value. The low substrate affinities of D296A and D296N are accompanied by decreased catalytic efficiencies for these mutants (k_{cat}/K_m values are 0.001 and 1% of that for the wild-type, respectively).

The crystal structure of D296A shows that the alanine substitution at position 296 has resulted in the disruption of the hydrogen bond between the carboxylate at 296 and N7 of purine riboside originally observed in the wild-type structure (compare Figures 6 and 8). Losing this hydrogen bond to the enzyme results in a 0.4 Å shift in the position of the purine ring and causes considerable destabilization of the substrate in the active site, as the kinetic data also suggest. This is reflected in the difference between the binding energies of the D296A mutant and the wild-type ($\Delta\Delta G_B = -2.5$ kcal/mol), which falls within the range of the typical energetic "value" of a hydrogen bond (0.5−5 kcal/mol; Fersht, 1985; Moody & Wilkinson, 1990). The higher affinity for adenosine and adenosine analogues exhibited by the D296N mutant compared to that exhibited by the D296A mutant may imply that some type of hydrogen bonding exists between one of the amide hydrogens of asparagine and N7. Such an interaction cannot be as strong as the H bond found between N7 and the wild-type Asp OH, since the difference in the free energy of binding of adenosine between the D296N mutant and the wild-type is about −1.4 kcal/mol. However, even if the nitrogen lone pair on N7 is delocalized by participating in a weak vs a strong hydrogen bond, this interaction is important, as the much better ability of D296N compared to that of D296A in binding and turning over substrate manifests. By comparison, a mutation that does not destabilize the enzyme−substrate interaction such as D295E results in negligible $\Delta\Delta G_B$ values (−0.1 kcal/mol).

It was surprising that purine riboside was a 10-fold less effective inhibitor of the D296N mutant and a 3-fold worse inhibitor of the D296A mutant than N_6-methyladenosine, when both compounds exhibit similar K_i values in the wild-type and D295E mutant enzymes (Table 2). N_6-Methyladenosine is a poorly catalyzed ADA substrate with a K_m of 5−11 μM and a k_{cat} of 0.3 s^{-1} (Zielke & Suelter, 1971; Porter & Spector, 1993). Purine riboside is an inhibitor of the enzyme with a K_i of 6.5 μM (Frieden et al., 1980). The absence of a substituent on C6 of this compound precludes its conversion into product. The similarity in K_m values between C6-substituted and unsubstituted purines has been interpreted as evidence that this portion of the substrate does not contribute to substrate specificity (Zielke & Suelter, 1971; Kurz & Frieden, 1987). Our K_i and K_m values for wild-type ADA and D295E corroborate this interpretation; it is therefore intriguing that N6MA behaves so very differently from PR in the Asp 296 mutants. From its K_i value, N6MA binds these mutants as well as the normal substrate adenosine does, but PR, lacking a C6 substituent, competes much less effectively with the substrate for binding. It appears that a substituted C6 on a substrate or inhibitor makes favorable binding contacts with the enzyme which become especially important when the strong hydrogen bond between Asp 296 and N7 is lost. PR, with no C6 substituent, and no way to form a hydrogen bond between its N7 and Asn 296 or Ala 296, can make fewer binding contacts with the enzyme and consequently becomes a much weaker inhibitor of adenosine than N6MA. The crystal structure of this mutant would help in clarifying the types of enzyme−substrate interactions in the active site.

Compared to those for the wild-type enzyme, the k_{cat} values for D296A and D296N are low (0.07 and 7%, respectively), but higher than the D295E value (0.05%). The aspartate 296 to alanine substitution absolutely abolishes the hydrogen bond with N7 and destabilizes the $\Delta G^{\ddagger}$ value by 4.0 kcal/mol. Clearly, the loss of this bond not only affects the ground state but also raises the energy barrier to the transition state. This is not surprising since all nitrogen lone pairs of adenosine are involved in hydrogen-bonding interactions, by which the aromaticity of the purine ring is reduced and formation of the tetrahedral intermediate facilitated (Wilson et al., 1991). Whatever the interaction may be between the mutant asparagine and the substrate in the ES complex, it must also stabilize the trnasition state to some extent, since the D296N mutant has a chemical activation step only 1.6 kcal/mol higher than that of the wild-type. By comparison, a mutation whose effects are seen in the transition rather than the ground state such as the aspartate 295 to glutamate yields a $\Delta\Delta G^{\ddagger}$ value of −4.6 kcal/mol.

The pH dependence of free wild-type ADA and the ADA−adenosine complex agrees with that seen in previous studies (Weiss et al., 1987; Sharff et al., 1992). An ionization constant of 5.5 is seen on the acidic limb of the profile and one of 8.5 on the basic limb. Originally, it had been suggested that the acidic ionization represented a carboxyl or histidyl group whereas the basic one a sulfhydryl residue (Kurz & Frieden, 1983; Weiss et al., 1987). We observed wild-type pH dependence for the D295E mutant-free enzyme (log k_{cat}/K_m) and the enzyme−substrate (log k_{cat}) complex (Figure 5). This is not surprising, since Asp 295 has its Oδ2 coordinated to the zinc and its Oδ1 participating in hydrogen bonds with the catalytic water and the OH of Ser 265 (Wilson & Quiocho, 1993). Thus, this residue is predicted to be more acidic than normal, i.e. to have a lower pK_a than 4, and certainly lower than the acidic pK_a of 5.5 we see in the ADA pH profile. The engineered Glu at this position is also expected to have a pK_a lower than 4, since it is able to coordinate the zinc as its crystal structure shows (Figure 7). The reason that we see any catalytic activity at all in the mutant enzyme is that, on rare occasions, a water molecule is able to fit in the proper place in the active site and become deprotonated by His 238 to form a hydroxylate. When this occurs, the environment surrounding the zinc consists of the Glu 295 vs the Asp, the catalytic water/hydroxylate, the three His ligands, and Glu 217 and His 238 (the primary catalytic residues). Thus, the mutant active site is now equivalent to the wild-type active site, and the pH dependence for the reaction is unchanged. Consequently, our pH profiles from pH 4.0 to 10.0 would not be expected to change as a result of the D295E mutation. This result is in agreement with the primary role of Asp 295 being that of coordinating the metal cofactor and orienting the catalytic water for attack in synergy with His 238 and the zinc.

From the crystal structure, Asp 296 is embedded in a highly hydrophobic environment, in close proximity to three Phe residues. Therefore, it is thought to be protonated and able to donate a hydrogen bond to N7 of the substrate. Its pK_a is thus expected to be much higher than 4.0, and probably higher than 7.0; deprotonation of this residue would result in less tight substrate binding and a decrease in the catalytic activity. Ionization constants from pH 6.0 to above 8.0 have been reported for protnated carboxyl groups in enzymes

(Tipton & Dixon, 1983; Fersht, 1985). If either the acidic pK_a of 5.5 or the basic pK_a of 8.5 in the wild-type enzyme represented the deprotonation of this aspartate, we would expect to see a grossly altered pH profile with our Asp 296 mutants. However, our pH profiles do not support this theory (Figure 5). The D296A-free enzyme and enzyme−substrate pH profile is identical to the wild-type profile in both the basic and acidic limbs. In the case of the D296N mutant, both of its profiles show elevated k_{cat} and k_{cat}/K_m values at pH 5.5 relative to the wild-type profile, perhaps because at those pH values N7 of the substrate can be protonated by the solvent. Protonation at N7 of imidazole rings is favorable due to resonance stabilization within the ring. Such protonation would have the same effect that the N7−D296 hydrogen bond has: it would reduce the aromaticity of the substrate's purine ring and enhance its catalysis by the D296N mutant. It appears then that, even if neither of the pK_a values reflects solely the ionization of Asp 296, they can be affected by mutations at this position, as is the case with D296N. Our pH stability experiments rule out the possibility that the activity decrease at the acidic or basic ends of the pH range is simply caused by the denaturation of either wild-type or mutant ADA.

We have changed residues 295 and 296 of the active site, and neither the basic nor the acidic pK_a is affected. Kati and Wolfenden (1989a) have discussed the possibility for the pK_a for N1 of the substrate approaching 5.1 in the lowest excited triplet state; since Glu 217 is the residue proposed to donate a proton to N1, its pK_a should be close to that value as well. Mutations on Glu 217 do not allow us to assign the acidic pK_a of 5.5 to theat residue unambiguously (Mohamedali et al., 1996). An alanine mutation on the other important active site group, His 238, shows a significant increase in k_{cat} at pH 5.5 compared to that at pH 7.0; however, an arginine mutation at this position leaves the pH profile unaltered. The basic pK_a of 8.5 has been attributed to a sulfhydryl ionization. Nevertheless, our work with Cys 262 mutants clearly excludes at least this sulfhydryl. From available data to date, it is difficult to attribute either of the two pK_a values solely to a specific active site residue. Rather, it appears that these values are combinations of ionization constants of multiple groups, since some of our mutations can clearly affect them.

From a structural point of view, a first indication that all three mutants were correctly folded and had no drastic tertiary structure abnormalities was that they eluted at times similar to those of wild-type from the ion-exchange and hydrophobic chromatography columns and reacted with antiserum against mouse ADA. The three mutants exhibited wild-type secondary structures based on circular dichroism spectra and similar tertiary folds as judged by fluorescence and near-UV CD spectroscopy. In the case of the D295E and D296A mutants, the crystal structures provided solid evidence for the overall retention of the wild-type secondary and tertiary fold. The only differences between the structures of these mutants and wild-type ADA were seen in the immediate vicinity of the mutations as discussed above.

Overall, our results support predictions for the roles of the two conserved neighboring aspartates 295 and 296 in the catalytic mechanism of ADA based on the crystallographic analysis. Aspartate 295 is not necessary for substrate binding or stabilization, but it is indispensable to the enzyme by virtue of its coordination to the zinc and correct positioning of the catalytic water molecule for subsequent deprotonation and attack. A longer glutamate residue can still coordinate the zinc, but is too long to allow the catalytic water to bind, and abolishes the enzyme's catalytic activity. Aspartate 296 is required for substrate binding, donating a hydrogen bond to N7 of the purine. Changing this residue into an alanine removes this bond, resulting in minimal substrate affinities. Replacing it with an asparagine, however, is not so drastic a change: affinities for substrate are still decreased, but less so than in the alanine mutant. In the absence of the N7−Asp 296 hydrogen bond, interaction between the enzyme and other parts of the substrate, such as the C6 substituent become important. Neither Asp 295 nor Asp 296 is responsible for the pK_a values observed when the pH dependence of the ADA reaction is tested. We conclude that both aspartates are essential to the proper catalytic behavior of ADA.

ACKNOWLEDGMENT

We thank the laboratories of Dr. John S. Olson and Dr. Kathleen Shive Matthews at Rice University for assistance with the circular dichroism and fluorimetry experiments; the laboratory of Dr. David Giedroc, Texas A&M University, for our FAAS experiments; Sandra Clark for performing all protein purifications; Ting Chi Liu for assistance with inhibition and kinetics studies; and Dr. Bruce F. Cooper for his helpful discussions.

REFERENCES

Adler, A. J., Greenfield, N. J., & Fasman, G. D. (1973) *Methods Enzymol. 27*, 675−735.
Auld, D. S. (1988) *Methods Enzymol. 158*, 13−14.
Bradford, M. (1976) *Anal. Biochem. 72*, 248−254.
Brünger, A. T. (1992) in *XPLOR: A System for Crystallography and NMR Version 3.1 Manual*, Yale University Press, New Haven, CT.
Callebaut, C., Krust, B., Jacotot, F., & Hovanessian, A. G. (1993) *Science 262*, 2045−2050.
Centelles, J. J., Franco, R., & Bozal, J. (1988) *J. Neurosci. Res. 19*, 258−267.
Chang, Z. (1992) Ph.D. Thesis, Baylor College of Medicine, Houston, TX.
Chang, Z., Nygaard, P., Chinault, A. C., & Kellems, R. E. (1991) *Biochemistry 30*, 2273−2280.
Cowan, M. C., Brady, R. O., & Widder, K. J. (1983) *Proc. Natl. Acad. Sci. U.S.A. 83*, 1089−1091.
Fersht, A. (1985) in *Enzyme Structure and Mechanism*, 2nd ed., pp 296−299, W. H. Freeman & Company, New York.
Frick, L., Neela, J. P., & Wolfenden, R. (1987) *Bioorg. Chem. 15*, 100−108.
Frieden, C., Kurz, L. C., & Gilbert, H. R. (1980) *Biochemistry 19*, 5303−5309.
Gan, T. E., Dadonna, P. E., & Mitchell, B. S. (1987) *Blood 69*, 1376−1380.
Glazer, R. (1980) in *Reviews on Drug Metabolism and Drug Interactions*, Vol. III, pp 105−128, Freund Publishing House, Ltd., London.
Hershfield, M. S., & Mitchell, B. S. (1995) in *The Metabolic and Molecular Basis of Inherited Disease* (Scrivner et al., Eds.) Vol. 1, pp 1725−1768, McGraw-Hill Inc., New York.
Jones, W., Kurz, L. C., & Wolfenden, R. (1989) *Biochemistry 28*, 1242−1247.
Kameoka, J., Tanaka, T., Nojima, Y., Schlossman, S. F., & Morimoto, C. (1993) *Science 261*, 466−469.
Kanno, H., Tani, K., Fujii, H., Iguchi-Ariga, S. M. M., Ariga, H., Kozaki, T., & Miwa, S. (1988) *Jpn. J. Exp. Med.*, 1−8.
Kati, W. M., & Wolfenden, R. (1989a) *Biochemistry 28*, 7919−7927.
Kati, W. M., & Wolfenden, R. (1989b) *Science 243*, 1591−1593.

Kunkel, T. A., Roberts, J. D., & Zakour, R. A. (1987) *Methods Enzymol. 154*, 367−382.
Kurz, L. C., & Frieden, C. (1983) *Biochemistry 22*, 382−389.
Kurz, L. C., & Frieden, C. (1987) *Biochemistry 26*, 8450−8457.
Kurz, L. C., LaZard, D., & Frieden, C. (1985) *Biochemistry 24*, 1342−1347.
Kurz, L. C., Moix, L., Riley, M. C., & Frieden, C. (1992) *Biochemistry 31*, 39−48.
Laemmli, U. K. (1970) *Nature 227*, 680−685.
Mohamedali, K. A., Kurz, L. C., & Rudolph, F. B. (1996) *Biochemistry 35*, 1672−1680.
Moody, P. C. E., & Wilkinson, A. J. (1990) in *Protein Engineering* (Rickwood, D., & Male, D., Eds.) pp 39−42, IRL Press at Oxford University Press, Oxford, U.K.
Pace, C. N., Shirley, B. A., & Thomson, J. A. (1990) in *Protein Structure* (Creighton, T.E., Ed.) pp 311−329, IRL Press at Oxford University Press, Oxford, U.K.
Philips, A. V., Robbins, D. J., & Coleman, M. S. (1987) *Biochemistry 26*, 2893−2903.
Porter, D. J. T., & Spector, T. (1993) *J. Biol. Chem. 268*, 2480−2485.
Renouf, J. A., Wood, A., Frazer, I. H., Thong, Y. H., & Chalmers, A. H. (1989) *Clin. Chem. 35*, 1478−1481.
Sharff, A. J., Wilson, D. K., Chang, Z., & Quiocho, F. A. (1992) *J. Mol. Biol. 226*, 917−921.
Tipton, K. F., & Dixon, H. B. F. (1983) in *Contemporary Enzyme Kinetics and Mechanism* (Purich, D. L., Ed.) Academic Press, New York.
Vallee, B. L., & Auld, D. S. (1990) *Proc. Natl. Acad. Sci. U.S.A. 87*, 220−224.
Weiss, P. M., Cook, P. F., Hermes, J. D., & Cleland, W. W. (1987) *Biochemistry 26*, 7378−7384.
Wilson, D. K., & Quiocho, F. A. (1993) *Biochemistry 32*, 1689−1693.
Wilson, D. K., Rudolph, F. B., & Quiocho, F. A. (1991) *Science 252*, 1278−1284.
Zielke, C. L., & Suelter, C. H. (1971) in *The Enzymes* (Boyer, P. D., Ed.) Vol. 4, pp 47−48, Academic Press, New York.

BI952920D